Proceedings of ICFA Mini-Workshop on Impedances and Beam Instabilities in Particle Accelerators, Benevento, Italy, 18-22 September 2017, CERN Yellow Reports: Conference Proceedings, Vol. 1/2018, CERN-2018-003-CP (CERN, Geneva, 2018)

MODELING OF FAST BEAM-ION INSTABILITIES*

L. Mether†, EPFL, Lausanne, Switzerland
A. Oeftiger, G. Rumolo, CERN, Geneva, Switzerland

Abstract

Beam-induced ionisation of residual gas in the vacuum chamber generates ions, which in an electron machine can accumulate around a passing bunch train. If the density of trapped ions becomes sufficiently high, a fast beam-ion instability will be excited. The development of the instability can be prevented by keeping the pressure of the residual gas below a certain value. This contribution describes the modeling of fast beam-ion instabilities and presents simulation studies of ion trapping and the evolution of the instability in the FCC-ee. Threshold ion densities for exciting the instability are estimated in order to deduce acceptable vacuum pressures for operation.

INTRODUCTION

The presence of residual gas in the vacuum chamber of a particle beam leads to the formation of electrons and ions through beam-induced ionisation. In the case of an electron beam, the generated electrons will be repelled by the beam and move towards the chamber walls, whereas ions are accelerated towards the centre of the chamber by the attractive beam force. The ions may be trapped by subsequent bunches and oscillate around the bunch train centroid, or be over-focused and lost on the walls if the kick from the beam is sufficiently strong. If a significant ion density builds up along the bunch train, coherent motion of the beam ensues and a fast beam-ion instability develops [1].

Ion trapping depends on several machine and beam parameters, as well as on the composition of the residual gas. A trapping condition can be derived from the linear approximation of the Bassetti-Erskine formula [2] for the field of a Gaussian beam and the stability condition of a linear beam trajectory. Ions of mass number A are trapped if

$$A > A_{\mathrm{tr}_{x,y}} = \frac{N r_p \Delta T_b c}{2\sigma_{x,y}(\sigma_x + \sigma_y)}\,, \qquad (1)$$

where r_p is the classical proton radius and c is the speed of light. The trapping mass number A_{tr_i} depends on the bunch spacing ΔT_b, the bunch intensity N, and the transverse beam sizes σ_x and σ_y. For an ion to be trapped, its mass number must be larger than the trapping mass number of both transverse planes. For flat bunches, typical in electron machines, the beam field and the induced kick on the ions are stronger in the vertical plane. Hence the instability occurs in the vertical plane and the trapping mass number is determined by the vertical condition.

If ions of mass number A are trapped along a train of bunches according to Eq. (1), the rise time of the induced instability for bunch number n_b can be written as

$$\tau^{i\,2}_{x,y} \propto \frac{\gamma^2 A \omega_\beta}{n_b^4 N^3 P^2 T_b c} \left(\sigma_x + \sigma_y\right)^3 \sigma^3_{x,y}\,, \qquad (2)$$

where ω_β is the betatron frequency. The instability develops faster for larger residual gas pressures P as well as for larger bunch numbers, i.e. the instability sets in at the tail of the bunch train. Furthermore, for a given pressure, the instability develops faster for smaller ion mass numbers, as long as the ions are trapped.

The results reviewed above are based on the linear approximation of the beam field, which underestimates ion trapping by overestimating the kick on ions outside of the core of the beam. With the full beam field, ions may be trapped and influence the beam even if their mass number is below the trapping mass number Eq. (1). In this contribution we present numerical simulations of the fast beam-ion instability in the electron ring of the FCC-ee, which is under design within the future circular collider project [3]. Ion trapping for mass numbers above and below the trapping mass is studied and the effect of the ions on the beam is compared in the two regimes. Viable partial pressures for common vacuum species are identified and mitigation strategies are discussed.

MACHINE PARAMETERS

The FCC-ee may be vulnerable to the fast beam-ion instability in particular at Z-pole operation due to the large number of bunches foreseen for operation in this mode. Selected design parameters at the time of this study are summarised in Table 1. The operational bunch spacing has not yet been fixed in the machine design. Here we use a bunch spacing ΔT_b of 2.5 ns which is the shortest considered spacing and hence the most critical for the fast beam-ion instability.

Table 1: FCC-ee parameters for Z production

Parameter	Symbol, Unit	Value
Energy	E [GeV]	45.6
Circumference	C [m]	97749.14
Bunch intensity	N	1.7×10^{11}
Geometric hor. emittance	ε_x [nm]	0.27
Geometric ver. emittance	ε_y [pm]	1.0
Bunch length	σ_z [mm]	3.5
Harmonic number	h_{RF}	130680
Number of bunches	[1/beam]	16640
Vertical damping time	τ_y^d [turns]	2533

* Work supported by the Swiss State Secretariat for Education, Research and Innovation, SERI
† lotta.mether@cern.ch

https://doi.org/10.23732/CYRCP-2018-001.63

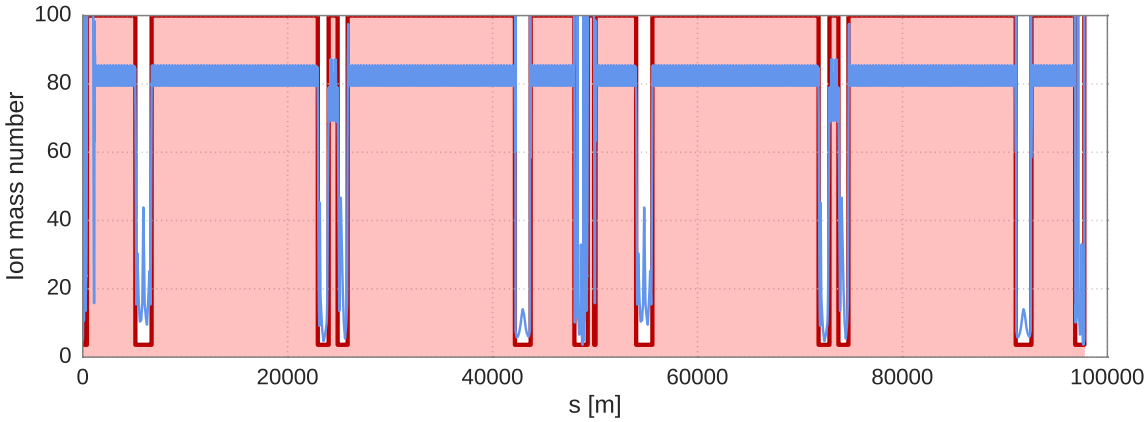

Figure 1: Trapping condition, Eq. 1, along the machine circumference. The trapping mass number for the real lattice is shown in blue and for the model of the straight sections in red.

For the study we consider the following residual gas species: H_2, CO and CO_2, with mass numbers and ionization cross-sections [4], σ, as indicated in Table 2. In order to study the trapping of different mass numbers and to determine individual partial pressure thresholds for the instability, each species is simulated independently.

Table 2: Residual gas species

Species	**A**	σ **[MBarn]**
H_2	2	0.5
CO	28	2.0
CO_2	44	2.0

SIMULATION MODEL

The simulations have been performed using the PyECLOUD and PyHEADTAIL macro-particle tracking tools [5, 6], with the following method based on the FASTION code [7, 8]. The machine lattice is divided into a number of segments, each of which is represented by an interaction point where the beam-ion interaction along the segment is modelled in 2D. Ions are generated bunch by bunch, and the beam-ion interaction is simulated separately for each bunch along the train.

The simulations are done in the strong-strong regime, where both the beam and the ion cloud are represented by sets of macro-particles. This allows us to model not only the bunch centroid motion, but also emittance growth and other multi-particle effects. The ion macro-particles are regenerated in every interaction point, whereas the beam macro-particles, defined by their phase space variables, are transported between the interaction points using the linear transverse transfer matrices. Synchrotron radiation damping has not been included in the simulation model, instead we compare the rise times found in the simulations to the vertical damping time of the machine (see Table 1).

Since the dynamics of the beam-ion interaction are highly sensitive to the transverse beam size, the ions are kicked with different strengths in different locations of the machine, according to the optics functions. Ideally the number of segments and interaction points would be chosen such that the machine lattice is comprehensively sampled. For a machine of the size of the FCC, however, this is not viable within a reasonable computation time. Instead, we model the machine using a smooth approximation with identical lattice functions in all segments and determine the required number of segments based on a convergence scan.

Because the lattice functions vary widely between the arcs of the machine and the straight sections, the two cases are simulated independently. This approach allows us to determine in which parts of the machine the pressure limits are more stringent, as well as to compare the trapping of various ion species at two different beam sizes. The arcs, which cover 86.6% of the machine, are modelled with a smooth approximation over the entire circumference with equal distances and phase advances between segments. To model the 13.4% of straight sections, each individual straight section is divided into a number of equidistant interaction points, while the arcs simply transport the beam between straight sections. To account for the different phase advances covered by the various straight sections, the phase advance between segments varies for each straight section. In both cases the lattice functions are selected to give the lowest trapping mass number within the corresponding part of the machine. The linear trapping condition along the machine circumference is shown in Fig. 1 in blue. The red curve shows the trapping mass in the model of the straight sections. A study of the number of kicks and segments needed in the arcs shows good convergence as of around 500 kicks. In the straight sections the number is scaled with respect to the length to 80 kicks per turn.

From Fig. 1 we can see that none of the ion species under study are trapped by the beam in the arcs of the machine, according to the trapping condition Eq. (1). In the straight sections, on the other hand, both CO and CO_2 are trapped according to Eq. (1), while H_2 remains below the trapping mass. As will be evident from the simulation results in the

following sections, some ions do in reality stay trapped along at least a part of the bunch train also in the arcs. However, they are less strongly trapped than in the straight sections, where the trapping mass number is significantly lower.

Due to the heavy computational burden of the simulations, only a limited number of bunches and turns can be simulated within a reasonable time. For the studies presented here, bunch trains of 50–200 bunches have been studied over 50 turns around the machine. Over this time, the expected vertical damping due to synchrotron radiation is 4 %. The individual gas pressures have been scanned from the pTorr range to a few tens of nTorr.

H_2 TRAPPING AND BEAM STABILITY

Figure 2 shows the impact of hydrogen gas in the arcs on a train of 50 bunches over 50 turns. Even for two relatively high pressures only a very marginal effect on the bunch train can be seen. In particular, the rate of emittance growth shown in Fig. 2b is slower than the expected shrinkage due to synchrotron radiation damping. Hence we do not expect hydrogen to cause any problems in the arcs of the machine for partial pressures up to 10 nTorr. These results are consistent with the expectations from the trapping condition, Eq. (1), and indicate that H_2^+ ions are not trapped in significant amounts along the bunch train.

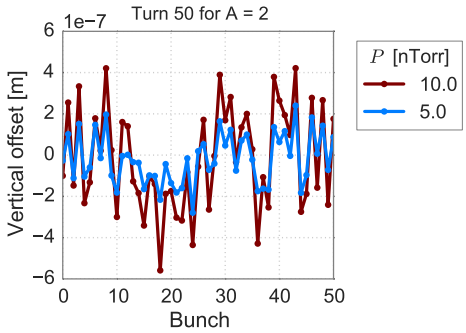

(a) Vertical bunch centroid offsets after 50 turns.

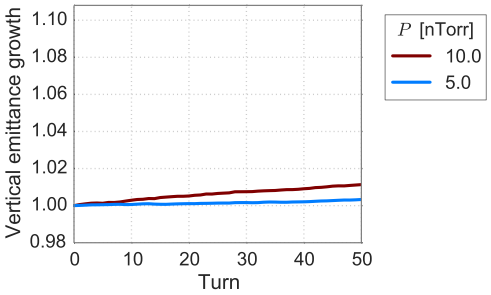

(b) Vertical emittance growth of most unstable bunch.

Figure 2: Bunch train evolution with selected pressures of H_2 ($A = 2$) gas in the arcs.

In contrast, in the straight sections, which have a much lower trapping mass number due to the higher beta functions, hydrogen ions do have a significant effect on the beam, although they are not trapped according to Eq. (1). The effect of hydrogen gas in the straight sections on a train of 50 bunches over 50 turns is shown in Fig. 3. While the ions receive smaller kicks in the straight sections due to the weaker beam fields compared to the arcs, the consequently increased trapping allows for more ions to accumulate along the bunch train, with a noticeable effect on the beam. Within 50 turns, excitation of centroid motion sets in at a pressure of 0.5 nTorr, whereas significant emittance growth is observed from pressures of 3 nTorr.

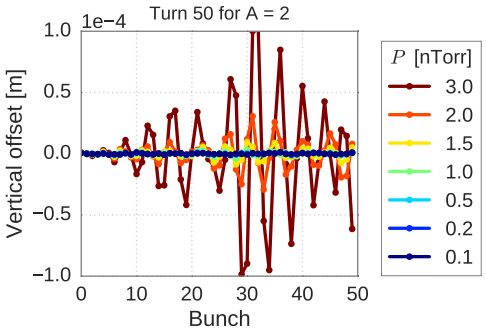

(a) Vertical bunch centroid offsets after 50 turns.

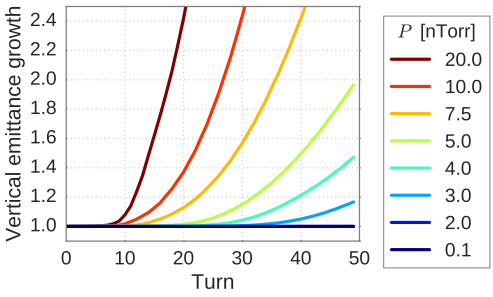

(b) Vertical emittance growth of most unstable bunch.

Figure 3: Bunch train evolution with selected pressures of H_2 ($A = 2$) gas in the straight sections. Note that the two graphs display different pressures.

CO AND CO_2 TRAPPING AND BEAM STABILITY

Figures 4a and 4b show the vertical centroid displacements of a train of 50 bunches after 50 turns with respectively CO and CO_2 gas in the arcs. The factor of vertical emittance growth (excluding the effect of radiation damping) for the most unstable bunch along the train is shown in Fig 5. Although the mass numbers of both species are well below the trapping mass number for the arcs, they are significantly heavier than hydrogen and are clearly able to generate fast beam-ion instabilities in the arcs.

The lowest pressure leading to significant centroid displacement is 0.2 nTorr for CO and 0.05 nTorr for CO_2, whereas emittance growth occurs from 0.5 nTorr for CO and from 0.1 nTorr for CO_2. Indeed, we can observe that the effect on the beam is stronger for CO_2 than for CO. For any given pressure, the instability sets in after fewer turns and grows faster for CO_2 compared to CO. This behaviour is

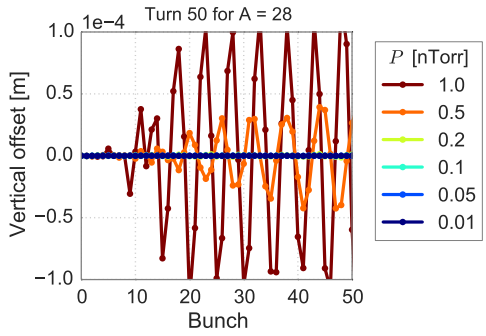

(a) Carbon monoxide ($A = 28$).

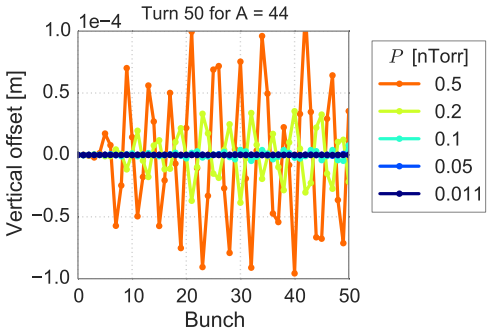

(b) Carbon dioxide ($A = 44$).

Figure 4: Vertical bunch centroid offsets after 50 turns with selected pressures of CO and CO_2 gas in the arcs.

contrary to what would be expected for strongly trapped ions, Eq. (2), where a faster developing instability is predicted for smaller mass numbers, and indicates qualitatively different instability dynamics when ions are not fully trapped.

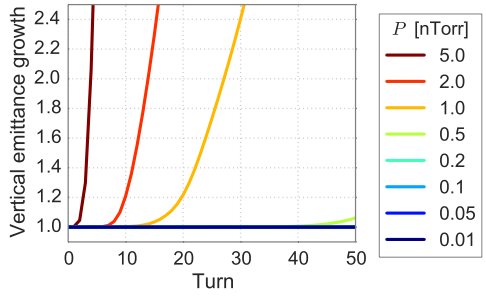

(a) Carbon monoxide ($A = 28$).

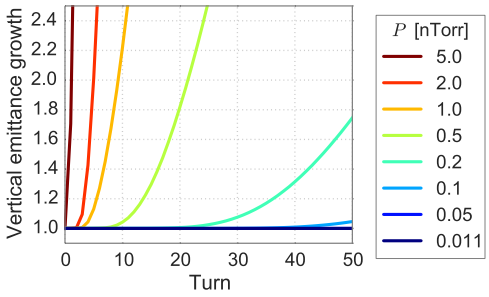

(b) Carbon dioxide ($A = 44$).

Figure 5: Vertical emittance growth of the most unstable bunch for CO and CO_2 gas in the arcs.

In the straight sections both species are expected to be trapped along the beam and give rise to fast beam-ion instabilities. This is confirmed by Fig 6, which displays the vertical centroid offsets across a bunch train after 50 turns with CO and CO_2 gas in the straight sections, respectively. The lowest pressure leading to significant centroid displacement is 10 pTorr for both species.

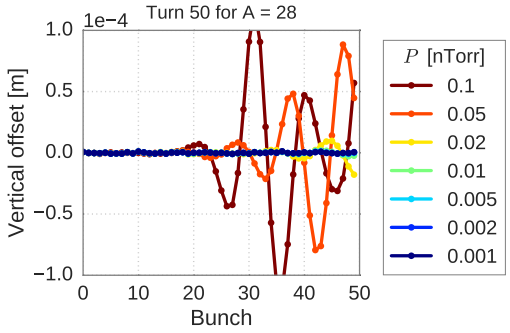

(a) Carbon monoxide ($A = 28$).

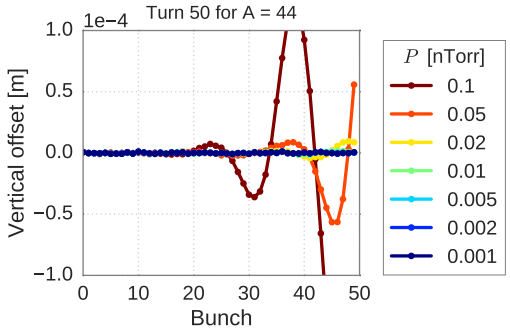

(b) Carbon dioxide ($A = 44$).

Figure 6: Vertical bunch centroid offsets after 50 turns with selected pressures of CO and CO_2 gas in the straight sections.

WEAK VERSUS STRONG TRAPPING

In the straight sections, the threshold pressures lie more than an order of magnitude below the values in the arcs, although they cover only 13.4 % of the machine circumference, indicating a much stronger trapping of the ions in the straight sections. We can also observe a contrast in the dynamics of the instability between the arcs and the straight sections, as illustrated in Fig. 7. In the straight sections, the expected behaviour of a fast beam-ion instability due to ion trapping is observed: the instability first sets in at the tail of the bunch train, and after a given number of turns extends over an increasing part of the bunch train for increasing pressure, approaching the head of the train. This dynamical behaviour applies to both the vertical emittance (see Fig. 7b) and the centroid motion along the bunch train and is similar for both species.

In the arcs, on the other hand, as well as for hydrogen in the straight sections, an increase in emittance growth along the bunch train is observed only at the beginning of the train, with all trailing bunches experiencing a similar amount of

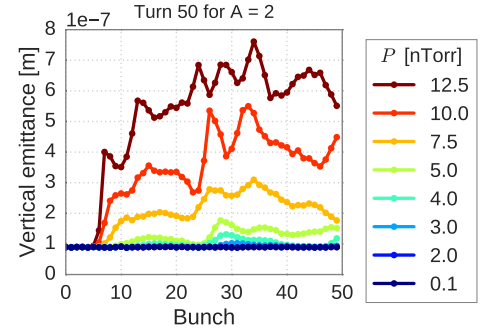

(a) Hydrogen ($A = 2$).

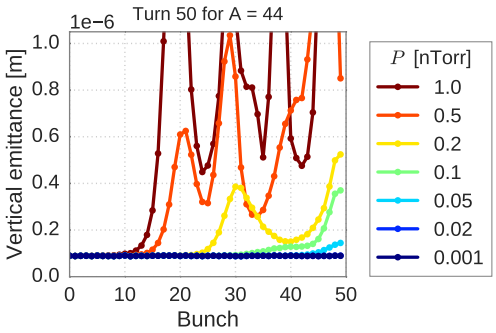

(b) Carbon dioxide ($A = 44$).

Figure 7: Vertical emittances of a bunch train after 50 turns with H_2 and CO_2 gas in the straight sections. Note that the two graphs display different pressures.

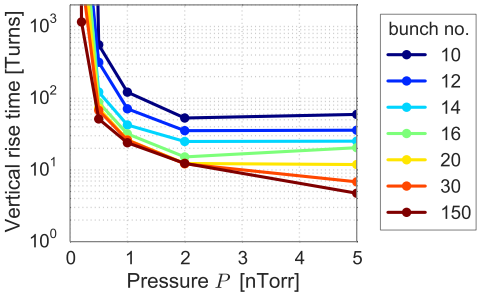

(a) Carbon monoxide ($A = 28$).

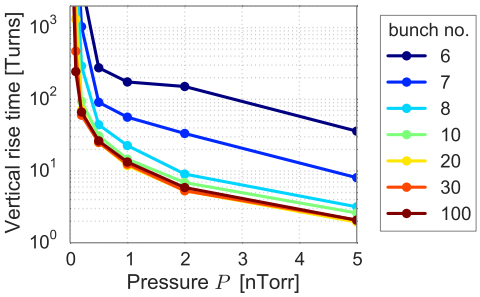

(b) Carbon dioxide ($A = 44$).

Figure 8: Vertical rise times for selected bunch numbers as a function of CO and CO_2 gas pressure in the arcs.

emittance growth (see Fig. 7a). This is illustrated also in Fig. 8, which shows the rise time of the instability (estimated from the emittance growth) for selected individual bunches along a train with CO and CO_2 gas, respectively. One can note that the rise time saturates after about 10-20 bunches and is essentially independent of the bunch number for most part of the train. This pattern is observed regardless of the residual gas pressure, the length of the bunch train, and the number of turns simulated — only the level of emittance growth that the train is saturated at varies depending on the pressure and the number of turns simulated. Also the envelope of the centroid motion along the bunch train exhibits a similar behaviour.

CONCLUSION

We can conclude that two different regimes for ion trapping have been observed with different consequences for beam stability, depending on the residual gas and beam parameters. When the trapping condition, Eq. (1), is satisfied, fast beam-ion instabilities with the behaviour expected from the linearised treatment occur. However, even when Eq. (1) is not fulfilled, ions can effectively be trapped and induce fast beam-ion instabilities. In our examples this occurs for H_2 in the straight sections and CO, and CO_2 in the arcs. In these cases the instability for a given ion mass and a given pressure is weaker than in the trapping regime, and also behaves qualitatively different. In particular, the evolution of the instability doesn't seem to depend on the number of preceding bunches in a train, except for the first 10-20 bunches. This behaviour could possibly be explained by limited trapping of the ions, which consequently might oscillate around the train only for a certain number of bunch passages before being lost. In the future, it would be interesting to study in more detail the ion behaviour in this non-linear regime, e.g. the typical ion-beam interaction length and how it varies with the ion mass, as well as the frequencies involved in the instabilities, which are related to the non-linear ion oscillations.

Table 3: Pressure thresholds for residual gas species

	H_2	**CO**	**CO_2**
Arc model	—	0.1 nTorr	0.02 nTorr
Straight sections	0.2 nTorr	5 pTorr	5 pTorr

The highest pressures found to be stable over 50 bunches and 50 turns for each considered species in the arcs and straight sections are summarised in Table 3. These values correspond to the allowed partial pressures for each species, with eventual constraints on the total pressure depending on the composition of the residual gas. In case the constraints presented here cannot be fulfilled by the vacuum system, there are several mitigation strategies that can be employed in order to relax them.

A standard mitigation strategy for the fast beam-ion instability is the inclusion od clearing gaps. However, the specific behaviour of the partly trapped species implies that, in those cases, mitigation can only be achieved by going to very short trains of around 10 bunches or less. In the straight sections,

on the other hand, additional clearing gaps are expected to increase the threshold pressure. For this approach to raise the threshold pressure with a certain factor, however, the train length would need to be reduced by the same factor, which means only a limited gain can be achieved in this way.

A more promising strategy would be to increase the bunch spacing. According to the trapping condition, Eq. (1), the minimum trapped mass number is directly proportional to the bunch spacing, indicating that increasing the spacing reduces the amount of ion trapping. Based on an additional simulation case, a bunch spacing of 7.5 ns raises the threshold pressure with at least a factor 20 compared to 2.5 ns for CO_2 gas in the arcs. A similar effect can be expected to occur also for CO in the arcs and H_2 in the straight sections. However, the effect may not be as strong for the heavier species in the straight sections, since the trapping condition there is significantly lower. In the straight section model, both CO and CO_2 would still be strongly trapped for a bunch spacing of 17.5 ns, whereas 19.6 ns is the theoretical maximum spacing for the design number of bunches. To accurately determine the pressure constraints for any given bunch spacing, further studies sampling in detail the lattice functions in the straight sections should be performed.

Finally, since the fast beam-ion instability is a coupled-bunch instability with no significant intra-bunch motion, a bunch-by-bunch feedback can typically efficiently suppress the instability, see e.g. [9]. Since the rise times of the instability for the lowest unstable pressures are relatively long, as seen in Figs. 3 and 5, a feedback system with a damping time of 10–100 turns should be able to increase the pressure threshold by more than a factor of 10. However, it is not clear that a feedback system would prevent the emittance growth associated with ion trapping.

ACKNOWLEDGEMENTS

The authors would like to thank R. Kersevan for helpful discussions.

REFERENCES

[1] T. O. Raubenheimer and F. Zimmermann, “Fast beam-ion instability. I. Linear theory and simulations”, Phys. Rev. E 52, 5487–5498, 1995.

[2] M. Bassetti and G. Erskine, “Closed expression for the electrical field of a two-dimensional gaussian charge”, Technical Report, CERN-ISR-TH/80-06, 1980.

[3] F. Zimmermann *et al*, “FCC-ee Overview”, proceedings of HF2014, Beijing, China, paper THP3H1, 2014.

[4] A.G. Mathewson and S. Zhang, “Beam-Gas Ionisation Cross Sections at 7.0 TeV”, Technical Report, LHC-VAC/AGM, 1996.

[5] G. Iadarola *et al*, “Evolution of Python Tools for the Simulation of Electron Cloud Effects”, proceedings of IPAC’17, Copenhagen, Denmark, paper THPAB043, 2017.

[6] K. Li *et al*, “Code Development for Collective Effects”, proceedings of HB2016, Malmo, Sweden, paper WEAM3X01, 2016.

[7] G. Rumolo and D. Schulte, “Fast ion instability in the CLIC transfer line and main linac”, proceedings of EPAC’08, Genoa, Italy, 655–657, 2008.

[8] L. Mether, G. Iadarola and G. Rumolo, “Numerical Modeling of Fast Beam Ion Instabilities”, proceedings of HB2016, Malmo, Sweden, paper WEAM4X01, 2016.

[9] A. Chatterjee *et al*, ‘ ‘Fast ion instability at the Cornell Electron Storage Ring Test Accelerator”, Phys. Rev. ST Accel. Beams 18, 064402, 2015.